Table 2 Precision of test loop instrumentation

Measurement	Range	Accuracy
Speed	0 - 3000 rpm	± 1 rpm
Torque	0 - 20 lb.ft	± 0.01 lb.ft
System temperatures	0 - 150 °C	± 2 °C

Discussion

Figure 2 is the graphical presentation of the results obtained during tests and the results obtained by Eq. (2) for the S/R ratios and disk surface roughnesses tested. In the above equation the effect of surface roughness k_a is introduced. The shape of the curve is exactly the same as Daily and Nece (1960a) Eq. (1), but c_m changes for different disk surface roughnesses from 2.70×10^{-3} to 4.51×10^{-3}. It can be seen that as the S/R ratio increases, c_m increases too and in addition, as the disk surface roughness increases the curve is shifted upwards, giving higher values for c_m. In the case of disk surface roughness k_a of 0.0163 mm, the results obtained are identical to those predicted by Eq. (1). This indicates that the surface roughness of the disk that Daily and Nece (1960a) used for their tests was around 0.0163 mm.

The precision of measurement of parameters recorded for each test condition is described in Table 2. The percentage of the fractional error (Holman, 1994) varied between 1.53 and 1.54 for c_m between 2.5×10^{-3} and 4.5×10^{-3}. The tests were repeated 5 times for each S/R ratio, disk surface roughness, and flow combinations. In both cases—flow at centerline and flow at peripheral—as the disk surface roughness increases the curve is shifted upwards giving higher values for c_m. In addition, the c_m values at the peripheral flowrate were lower than at the centerline flowrate. Experiments from many researchers have indicated that an optimum S/R ratio exist giving a minimum c_m. This optimum ratio appeared to be between 0.010 to 0.015 for a Re of 10^6. Also, it was indicated that a second optimum S/R ratio may occur greater than the above S/R that will give also a second minimum value for c_m. At the centerline flow, the minimum value for the c_m appeared when the S/R ratio was at the minimum of 0.0133 verifying that for smaller S/R ratios an optimum ratio may exists. At the peripheral flow, the minimum value for c_m appeared when the S/R ratio was at the minimum of 0.0133 verifying once again that for smaller S/R ratios an optimum ratio may exist. Moreover a second optimum S/R ratio occurred at 0.0600 giving a second minimum value for c_m.

For the roughest disk with a surface roughness of 0.0261 mm the approximate theory calculation appeared to be between the experimental results with an error of −8.63 to 5.06 percent. Daily and Nece equation (1960) is well below the experimental results. The experimental results for the disk surface roughness of 0.0163 mm appeared to be lower than the approximate theory calculation with an error of 1.27 to 6.01 percent. Daily and Nece (1960) equation coincide with the approximate theory as explained before. For the disk with a surface roughness of 0.0083 mm the approximate theory calculation appeared to be between the experimental results, at the beginning, and then slightly higher with an error of 5.03 percent to −6.57 percent. Daily and Nece equation is well above the experimental results.

Conclusions

The following general conclusions may be drawn from this study, associated with the rotation of different surface roughnesses disks, and, in general, with disk friction losses occurring in centrifugal pumps:

(i) Disk friction coefficient c_m increases with the disk surface roughness k_a.

(ii) Disk friction coefficients c_m at the peripheral flowrate were lower than those on the centerline.

(iii) At the peripheral flow a second optimum S/R ratio of 0.0600 was observed.

(iv) Suggested empirical equations by other researchers agreed with experimental results only in the case of disk surface roughness of 0.0163 mm.

(v) The approximate solution leads to the empirical Eq. (2), which can predict the experimental results with an error of −8.63 to 6.01 percent.

References

Bennet, T. P., and Worster, R. C., 1960, "The Friction on Rotating Discs and the Effect on Next Radial Flow and Externally Applied Whirl," British Hydrodynamic Research Association.

Braske, U. M., 1975, "Investigations on the Pumping Effect of Rotating Discs," *Proceedings of the Institution of Mechanical Engineers*, Vol. 189, pp. 36–75.

Daily, J. W., and Nece, R. E., 1960a, "Roughness Effects on Frictional Resistance of Enclosed Rotating Discs," ASME JOURNAL OF BASIC ENGINEERING, Vol. 82, pp. 553–562.

Daily, J. W., and Nece, R. E., 1960b, "Chamber Dimension Effects on Induced Flow and Frictional Resistance of Enclosed Rotating Discs," ASME JOURNAL OF FLUIDS ENGINEERING, Vol. 82, pp. 217–232.

Goldstein, S., 1935, "On the Resistance to the Rotation of a Disc Immersed in a Fluid," *Proceedings of the Cambridge Philosophical Society*, Vol. 31, pp. 232–241.

Holman, J. P., 1994, Experimental Methods for Engineers, Sixth Edition, McGraw-Hill, New York.

Kurokawa, J., and Toyokura, T., 1976, "Axial Thrust, Disc Friction Torque and Leakage Loss of Radial Flow Turbomachinery," National Engineering Laboratory, International Conference on Pump and Turbine Design and Development, Paper 5-2.

Murata, S., Miyake, Y., and Iemoto, Y., 1976, "A Study on a Disc Friction Pump 1st Report," *Bulletin of the Japanese Society of Mechanical Engineers*, Vol. 19, No. 128, pp. 168–178.

Murata, S., Miyake, Y., and Iemoto, Y., 1976, "A Study on a Disc Friction Pump 2nd Report," *Bulletin of the Japanese Society of Mechanical Engineers*, Vol. 19, No. 236, pp. 160–171.

Osterwalder, J., 1978, "Efficiency Scale-Up for Hydraulic Turbomachines With Due Consideration of Surface Roughness," *Journal of Hydraulic Research*, Vol. 16, No. 1, pp. 55–76.

Poullikkas, A., 1991, "Disc Friction Study," Loughborough University of Technology, Department of Mechanical Engineering (internal report).

Schlichting, H., 1955, *Boundary Layer Theory*, McGraw-Hill, New York.

Stepanoff, J., 1948, *Centrifugal and Axial Flow Pumps*, Wiley, New York.

Varley, F. A., 1961, "Effects of Impeller Design and Surface Roughness on the Performance of Centrifugal Pumps," *Proceedings of the Institution of Mechanical Engineers*, Vol. 184, pp. 955–989.

Watabe, K., 1958, "On Fluid Friction of Rotational Rough Disc in Rough Vessel," *Bulletin of the Japanese Society of Mechanical Engineers*, Vol. 1, No. 1, pp. 68–74.

Watabe, K., 1965, "On Fluid Resistance of Enclosed Rotating Rough Discs," *Bulletin of the Japanese Society of Mechanical Engineers*, Vol. 8, No. 32, pp. 609–619.

Worster, R. C., 1957, "The Effects of Skin Friction and Roughness on the Losses in Centrifugal Pump Volutes," British Hydrodynamic Research Association.

A Note on the Baldwin-Lomax Turbulence Model

J. He[1] and J. D. A. Walker[1]

An analytic expression is obtained for the constant C_{cp} in the Baldwin-Lomax model by comparing self-similar solutions for velocity in a constant pressure incompressible flow that are

[1] Postdoctoral Fellow and Professor, respectively, Department of Mechanical Engineering and Mechanics, Lehigh University, Bethlehem, PA 18015.

Work supported by NASA grant NAE-1-832.

Contributed by the Fluids Engineering Division of THE AMERICAN SOCIETY OF MECHANICAL ENGINEERS. Manuscript received by the Fluids Engineering Division August 23, 1994; revised manuscript received December 16, 1994. Associate Technical Editor: G. Karniadakis.

based on the Cebeci-Smith and Baldwin-Lomax models; both models are shown to give identical results when the model C_{cp} has a specific analytical form.

I Introduction

In the numerical computation of turbulent boundary-layer flows, algebraic eddy viscosity models are often the most common choice in Navier-Stokes computer codes. Although such models are known to have certain deficiencies, their relative simplicity leads to minimum requirements in computer time and storage. In addition, the predicted results are often quite credible, at least for attached turbulent boundary layers on a smooth surface. Two formulations in extensive use are the Cebeci-Smith (1974) and Baldwin-Lomax (1978) models, which utilize the same mixing length model for the inner part of the boundary layer but a different eddy viscosity model in the outer part. The outer portion of the Cebeci-Smith model contains the displacement thickness δ^* as what is, in effect, a local representative length scale for the boundary layer. However, for a number of configurations, such as various internal flows or a boundary layer encountering a streamwise feature like a backward-facing step, the determination of δ^* can be problematic. For this reason, Baldwin and Lomax (1978) introduced another outer length scale and determined constants in the new model by comparison with numerical solutions for constant pressure boundary layers at transonic speeds produced using the Cebeci-Smith (1974) model. The model has been applied to a wide variety of two- and three-dimensional flows, with and without boundary layer separation (see, for example, Baldwin and Lomax, 1974; Visbal and Knight, 1984; King, 1987) with varying, but in many cases acceptable, levels of success.

Over the years, other suggestions have been put forward for the modeling constants in the Baldwin-Lomax model (see, for example, Visbal and Knight, 1984) and it has been hypothesized that a variation in the constants is necessary to account for compressibility with increasing mainstream Mach number M_∞. The question of compressibility will be addressed here subsequently. At transonic speeds, compressibility effects in a constant pressure boundary layer are relatively small when compared to a purely incompressible flow ($M_\infty \to 0$). In this note, a systematic way of determining the model constants in the Baldwin-Lomax (1978) model is described. It is shown that analytical solutions can be obtained for constant pressure turbulent boundary layers and with the appropriate choice of the model constants, both models give the identical solution. The resulting analytical formula give results that are close to those originally estimated by Baldwin and Lomax (1978). The present results may be of some utility in parametric studies, particularly in three-dimensional flows, where model constants are sometimes varied.

II Formulation

The equations governing a two-dimensional incompressible boundary layer at constant pressure may be written

$$u\frac{\partial u}{\partial x} + v\frac{\partial u}{\partial y} = \frac{\partial \tau}{\partial y}, \quad \frac{\partial u}{\partial x} + \frac{\partial v}{\partial y} = 0, \tag{1}$$

where τ is a total stress defined by

$$\tau = \sigma + \frac{1}{\mathrm{Re}}\frac{\partial u}{\partial y}, \quad \sigma = -\overline{u'v'}. \tag{2}$$

In these equations, all lengths and velocities are dimensionless with respect to a characteristic length L^*_{ref} and a speed U^*_{ref} and the Reynolds number is defined by $\mathrm{Re} = U^*_{\mathrm{ref}} L^*_{\mathrm{ref}}/\nu$, where ν is the kinematic viscosity. In an eddy viscosity model, the Reynolds stress is expressed in the form

$$-\rho\overline{u'v'} = \epsilon\frac{\partial u}{\partial y}, \tag{3}$$

where ϵ is the eddy viscosity function. In both the Cebeci-Smith and Baldwin-Lomax models, an inner eddy viscosity defined by

$$\epsilon_i = \rho(\kappa y D)^2|\omega|, \quad D = 1 - \exp(-y^+/A^+), \tag{4}$$

is used, where ρ is the density, κ is the von Karman constant, and $\omega = -\partial u/\partial y$ is the vorticity; thus the inner model is a mixing length model. In addition, D is the van Driest damping factor, where $A^+ = 26$ and y^+ is the scaled inner coordinate defined by

$$y^+ = \mathrm{Re}\, u_* y, \quad u_*^2 = \frac{1}{\mathrm{Re}}\frac{\partial u}{\partial y}\bigg|_{y=0}, \tag{5}$$

with u_* being the dimensionless friction velocity. In the outer region, an eddy viscosity formula is employed with

$$\epsilon_o = \rho K U_e \delta^* F_{kleb}, \quad F_{kleb} = \left\{1 + 5.5\left(\frac{y}{\delta}\right)^6\right\}^{-1}, \tag{6}$$

for the Cebeci-Smith model, where K is the Clauser constant having a value of 0.0168; U_e is the velocity at the boundary-layer edge, F_{kleb} is an intermittency correction, and δ is the boundary-layer thickness. The intermittency correction represents a curve fit which Klebanoff (1954) originally represented in terms of an error function. In the Baldwin-Lomax model, the outer eddy viscosity formula is

$$\epsilon_o = \rho K C_{cp} F_{\mathrm{wake}} F_{kleb}, \tag{7}$$

where again $K = 0.0168$, C_{cp} is a constant, and $F_{\mathrm{wake}} = y_{\max} F(y_{\max})$; here $y_{\max}$ denotes the location where the function

$$F = y|\partial u/\partial y|\, D, \tag{8}$$

reaches an absolute maximum. In addition, the intermittency factor is modified to the form

$$F_{kleb} = \left\{1 + 5.5\left(\frac{C_{kleb} y}{y_{\max}}\right)^6\right\}^{-1}, \tag{9}$$

where C_{kleb} is a constant. In both models the inner formula (4) is joined to either of the outer formula (6) or (7) at the location where both are equal. Baldwin and Lomax (1978) originally suggested values of $C_{cp} = 1.6$ and $C_{kleb} = 0.3$ and in subsequent work, other authors have used different values of the constants; for example, Visbal and Knight (1984) suggest $C_{cp} = 1.2$ and $C_{kleb} = 0.65$ for incompressible flow ($M_\infty \to 0$) and $C_{cp} = 2.08$ for an adiabatic supersonic flow at $M_\infty = 3$. A recent study by He et al. (1995) shows how the Baldwin-Lomax model can be extended to variable density flows with and without heat transfer well up into the low hypersonic range ($M_\infty \sim 10$) using universal values of the constants. Here the objective is to establish the base values of the modeling constants, and this is accomplished by a comparison of equilibrium velocity profiles in a constant pressure flow.

To start with, the intermittency portion of the model, F_{kleb}, will be taken equal to unity; this term is known to have very little effect on the shape of the velocity profile, or the critical features of the turbulence models. In the limit $\mathrm{Re} \to \infty$, it is well known that the turbulent boundary layer is a composite double layer consisting of an outer defect layer and an inner wall layer. In the outer layer, the velocity is of the form

$$u = U_e + u_* \frac{\partial F_1}{\partial \eta} + \ldots, \tag{10}$$

where the defect function $\partial F_1/\partial\eta$ is a function of the scaled

variable $\eta = y/\Delta_o$ for a self-similar flow, with $\Delta_o = \Delta_o(x, \mathrm{Re})$ proportional to the local boundary-layer thickness; for a constant pressure flow Δ_o can be defined by $\Delta_o = U_e\delta^*/u_*$ (Fendell, 1972). The defect function must satisfy the boundary conditions

$$\frac{dF_1}{d\eta} \sim \frac{1}{\kappa}\log\eta + C_o \quad \text{as} \quad \eta \to 0;$$

$$\frac{dF_1}{d\eta} \to 0 \quad \text{as} \quad \eta \to \infty, \tag{11}$$

where C_o is a constant. The first of these conditions is required to match the "law of the wall" in the wall-layer solution, while the second is the statement of matching to the external mainstream. In the wall layer, the velocity is a function of the scaled variable y^+ defined in Eq. (5), and the velocity profile is such that $u = u_*U^+(y^+) + \ldots$, with

$$U^+ = 0 \quad \text{at} \quad y^+ = 0,$$

$$U^+ \sim \frac{1}{\kappa}\log y^+ + C_i \quad \text{as} \quad y^+ \to \infty. \tag{12}$$

Here C_i is a constant generally supposed to have a universal value of $C_i = 5.0$. It is easily shown that the convective terms in Eq. (1) are negligible in the thin wall layer, which is therefore a constant stress layer with $\tau = \tau_w = u_*^2$. This serves to determine the equation for the velocity profile in the inner region, and with the model (4) it is easily verified that

$$\frac{dU^+}{dy^+} + \kappa^2 y^{+2}\mathcal{D}\left(\frac{dU^+}{dy^+}\right)^2 = 1, \tag{13}$$

which can be integrated using conditions (12) to find $U^+(y^+)$.

For large y^+, the damping factor $\mathcal{D}$ approaches unity and from Eq. (4), the inner eddy viscosity becomes linear in y^+. Thus the eddy viscosity for the outer part of the boundary layer may be written as $\epsilon = U_e\delta^*\hat{\epsilon}$ where $\hat{\epsilon}$ is the simple ramp function

$$\epsilon = \begin{cases} \chi, & \eta > \eta_m \\ \kappa\eta, & \eta \le \eta_m \end{cases}, \tag{14}$$

where $\eta_m = \chi/\kappa$, $\chi = K = 0.0168$ for the Cebeci-Smith model and $\chi = KC_{cp}y_{\max}F_{\max}/U_e\delta^*$ for the Baldwin-Lomax model. In the outer layer, the viscous stress in Eq. (2) is negligible, and it is easily shown that the defect function satisfies

$$\frac{d}{d\eta}\left\{\hat{\epsilon}\frac{d^2F_1}{d\eta^2}\right\} + \eta\frac{d^2F_1}{d\eta^2} = 0. \tag{15}$$

The solution satisfying conditions (11) is

$$\frac{dF_1}{d\eta} = \begin{cases} -\sqrt{\frac{\pi}{2\chi}}\, e^{-\chi/2\kappa^2}\,\mathrm{erfc}\left\{\sqrt{\frac{1}{2\chi}}\,\eta\right\}, & \eta > \eta_m, \\ -\frac{1}{\kappa}E_1\left(\frac{\eta}{\kappa}\right) + C_o - \frac{1}{\kappa}\{\gamma_o - \log\kappa\}, & \eta \le \eta_m, \end{cases} \tag{16}$$

where C_o is the outer region log-law constant given by

$$C_o = \frac{1}{\kappa}\left\{\gamma_o - \log\kappa + E_1(\chi/\kappa^2) - \sqrt{\frac{\pi}{2\chi}}\, e^{-K/2\kappa^2}\,\mathrm{erfc}\left\{\sqrt{\frac{\chi}{2\kappa^2}}\right\}\right\}. \tag{17}$$

In Eqs. (16) and (17) erfc and E_1 denote the complementary error function and exponential integral, respectively, and $\gamma_o = 0.577215\ldots$ is Euler's constant.

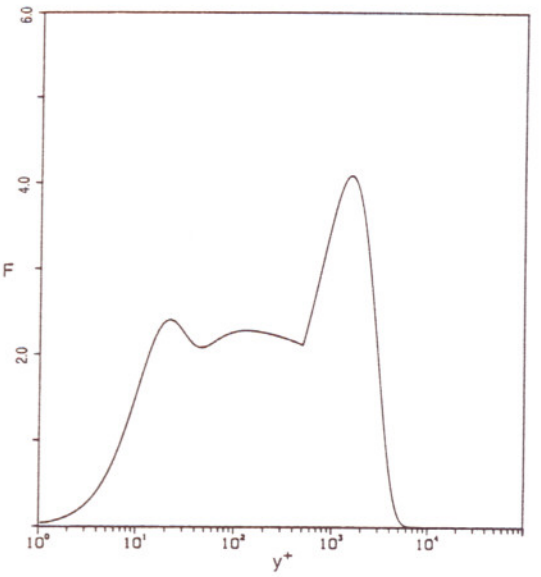

Fig. 1 Variation of F for a constant pressure boundary layer for $\mathrm{Re}_{\delta^*} = 10{,}000$

To determine the value of χ in Baldwin-Lomax model required to reproduce the Cebeci-Smith model, it is necessary to calculate the function F in Eq. (8). A composite profile for the entire boundary layer is formed as follows:

$$u = U_e + u_*\frac{dF_1}{d\eta} + u_*\left\{U^+ - \frac{1}{\kappa}\log y^+ - C_i\right\}, \tag{18}$$

and the function F is plotted in Fig. 1 for $\mathrm{Re}_{\delta^*} = 10{,}000$; here u_* is evaluated from the relation

$$\frac{U_e}{u_*} = \frac{1}{\kappa}\log\{\mathrm{Re}_{\delta^*}\} + C_i - C_o, \tag{19}$$

which must be satisfied so that the inner and outer profiles in Eqs. (10) and (12) match (Fendell, 1972); in addition, $\mathrm{Re}_{\delta^*} = \mathrm{Re}U_e\delta^*$. The corner in F shown in Fig. 1 near $y^+ \simeq 1000$ occurs at the point $\eta_m = \chi/\kappa$. It may be noted that an absolute maximum occurs in F in the outer part of the boundary layer, although local minima occur in the wall layer. For example, an extremum must occur in the overlap zone (for large y^+) in view of the last of conditions (12). However, if the absolute maximum is always selected, $y_{\max}$ occurs in the outer layer and can be chosen uniquely here and in flows with pressure gradient, except in some flows that involve separation (Visbal and Knight, 1984). Since the absolute maximum occurs in the outer layer, it suffices to examine the extrema of $F = \eta\partial u/\partial\eta$, and using Eq. (15), it is easily shown that

$$\eta\frac{d^2F_1}{d\eta^2} = \begin{cases} \frac{1}{\chi}\, e^{-\chi/2\kappa^2}\eta\,\exp(-\eta^2/2\chi), & \eta > \eta_m, \\ \frac{1}{\kappa}\exp(-\eta/\kappa), & \eta \le \eta_m. \end{cases} \tag{20}$$

Therefore the maximum occurs well into the outer part of the boundary layer, and it is easily shown that this occurs at $\eta_{\max} = \sqrt{\chi}$. The corresponding values of $F_{\max}$ and $y_{\max}$ are

$$F_{\max} = u_*\frac{1}{\sqrt{\chi}}\exp\left\{-\frac{1}{2}\left(1 + \frac{\chi}{\kappa^2}\right)\right\}, \quad y_{\max} = \frac{\sqrt{\chi}U_e\delta^*}{u_*}. \tag{21}$$

With χ defined for both models following Eq. (14), it may easily be verified that both models are equivalent if

$$C_{cp} = \exp\left\{\frac{1}{2}\left(1 + \frac{K}{\kappa^2}\right)\right\}. \quad (22)$$

Upon substituting $\kappa = 0.40$ and $K = 0.0168$, it follows that $C_{cp} = 1.738$, as compared to the original estimate $C_{cp} = 1.6$ (Baldwin and Lomax, 1978).

In obtaining the result (22), it has been assumed that the intermittency factor (9) is unity and it is of interest to determine if this factor has any significant influence on the location of η_{max}. Consider the equivalent of (15) in the outer region $\eta > \eta_m$ with the factor (9) included; this yields

$$\frac{d}{d\eta}\left\{\frac{\chi}{(1 + 5.5C_{kleb}^6\eta^6/\eta_{max}^6)}\frac{d^2F_1}{d\eta^2}\right\} + \eta\frac{d^2F_1}{d\eta^2} = 0, \quad (23)$$

which is considerably more difficult to integrate analytically. However, the value of η_{max} occurs where $\eta F_1''' + F_1'' = 0$, and using this and Eq. (23), it can be shown that the maximum is located at

$$\eta_{max} = \sqrt{\chi} + 16.5C_{kleb}^6\chi^{7/2}/\eta_{max}^6 + \ldots \quad (24)$$

Thus the maximum is shifted only a minuscule amount from the value $\eta_{max} = \sqrt{\chi}$ calculated when the intermittency correction is not used. Numerical solutions obtained with the intermittency correction show virtually no difference from the analytical solution (16). Thus there does not appear to be a basis for fixing C_{kleb} at a value different from that indicated by Baldwin and Lomax (1978).

III Conclusions

In the present note, an expression for the constant C_{cp} in the Baldwin-Lomax turbulence model has been determined analytically. With a base value of the constant established, the recent study by He et al. (1995) shows how this model (as well as the Cebeci-Smith model) can be extended to account for the effects of variable density in supersonic flow without any changes in the modeling constants.

References

Baldwin, B. L. and Lomax, H., 1978, "Thin-Layer Approximation and Algebraic Model for Turbulent Separated Flows" AIAA Paper 78-257, January.

Cebeci, T., and Smith, A. M. O., 1974, *Analysis of Turbulent Boundary Layers*, Academic Press, New York.

Fendell, F. E., 1972, "Singular Perturbation and Turbulent Shear Flow Near Walls," *Journal of the Astronautical Sciences*, Vol. 20, pp. 129–165.

He, J., Kazakia, J. Y., and Walker, J. D. A., 1994, "An Asymptotic Two-Layer Model for Supersonic Boundary Layers", *1995 Journal of Fluid Mechanics*, Vol. 25, pp. 159–198.

King, L. S., 1987, "A Comparison of Turbulence Closure Models for Transonic Flows About Airfoils," AIAA Paper 87-0418, Jan.

Klebanoff, P. S., 1954, "Characteristics of Turbulence in a Boundary Layer with Zero Pressure Gradient," NACA Tech. Note 3178.

Visbal, M. and Knight, D., 1984, "The Baldwin-Lomax Turbulence Model for Two-Dimensional Shock-Wave/Boundary-Layer Interactions" *AIAA Journal*, Vol. 22, pp. 921–928.

Stability of Computational Algorithms Used in Molecular Dynamics Simulations

Akira Satoh[1]

The present study focuses on a three-dimensional Lennard-Jones system in a thermodynamic equilibrium in order to discuss divergence processes, the relationship between time intervals and divergence times, and the influence of time intervals on thermodynamic quantities and transport coefficients under various number density and temperature. It is found that the velocities of molecules in a system gradually increase with time until the system suddenly diverges exponentially. The time interval-divergence time relationship can be expressed in approximate terms as linear functions if the data are plotted on logarithmic scales, and the system diverges more easily as temperature or number density increases. Thermodynamic quantities show the influence of large time intervals more clearly than do transport coefficients.

1 Introduction

Molecular dynamics (MD) is a molecular simulation method, and is a powerful tool for investigating physical phenomena at the microscopic level (Heermann, 1990). The appearance of supercomputers stimulates the application of MD methods to fluids engineering fields, such as to internal structures of shock waves in liquids (Holian et al., 1980; Holian, 1988; Tsai and Trevino, 1981; Satoh, 1993a), flow around a sphere (Satoh, 1993b), flow around a cylinder (Rapaport, 1987; Satoh, 1993c), Bénard cell problems (Mareschal et al., 1988), and flow in a two-dimensional duct (Mo and Rosenberger, 1991).

Computation time governs the successful application of MD methods to flow problems. These applications need to be extended to larger molecular systems. A reduction in computation time may be attained by adopting an algorithm which can use large time intervals, and by using more efficient techniques for calculating intermolecular forces. Although many computational algorithms have been presented, few studies have attempted to clarify the divergence properties of MD algorithms. Some studies discussed the relationship between energy fluctuations in systems and time intervals for various MD algorithms, while few studies discussed the relationship between divergence times and time intervals. Since divergence properties are not clearly understood in MD algorithms, the values for time intervals which have been empirically used for equilibrium simulations may also be adopted to simulate flow problems. If we simulate normal shock waves with such empirical time intervals, the results of number density profiles will seem reasonable, while pressure may be larger by some orders of magnitude. This is obviously due to too large time intervals, so that we cannot use the empirical time intervals used for thermodynamic equilibrium without sufficient reflection for flow problems.

The purpose of this study is to clarify the relationship between divergence processes and time intervals, and the dependencies of divergence times on time intervals. These results are expected to provide guidance in determining values of time intervals in actual simulations, and also in developing a new algorithm that will not diverge easily.

2 Microcanonical Ensemble Molecular Dynamics

2.1 Lennard-Jones System and Velocity Verlet Algorithm. We assume a model system with number density N and

[1] Department of Mechanical Engineering, Faculty of Engineering, Chiba University, 1-33, Yayoi-cho, Inage-ku, Chiba 263, Japan.

Contributed by the Fluids Engineering Division of THE AMERICAN SOCIETY OF MECHANICAL ENGINEERS. Manuscript received by the Fluids Engineering Division July 11, 1994; revised manuscript received January 20, 1995. Associate Technical Editor: J. A. C. Humphrey.